

Performance Analysis of Spatial Laser Speckle Contrast Implementations

Pedro G. Vaz^{1,2}, Anne Humeau-Heurtier², Edite Figueiras³, Carlos Correia¹ and João Cardoso¹

¹*LIBPhys-UC, Department of Physics, University of Coimbra, R. Larga, 3004-516 Coimbra, Portugal*

²*University of Angers, LARIS - Laboratoire Angevin de Recherche en Ingénierie des Systèmes,
62 avenue Notre-Dame du Lac, 49000 Angers, France*

³*International Iberian Nanotechnology Laboratory, Ultrafast Bio and Nanophotonics Group, Braga, Portugal*

Keywords: Laser Speckle Imaging, Spatial Contrast, Algorithm Implementation, MATLAB, Convolution.

Abstract: This work presents an analysis of the performances for four different implementations used to compute laser speckle contrast on images. Laser speckle contrast is a widely used imaging technique for biomedical applications. These implementations were tested using synthetic laser speckle patterns with different resolutions, speckle sizes, and contrasts. From the applied methods, three implementations are already known in the literature. A new alternative is proposed herein, which relies on two-dimensional convolutions, in order to improve the image processing time without compromising the contrast assessment. The proposed implementation achieves a processing time two orders of magnitude lower than the analytical evaluation. The goal of this technical manuscript is to help the developers and researchers in computing laser speckle contrast images.

1 INTRODUCTION

Laser speckle is an interference phenomenon that occurs when coherent light is used to illuminate a sample. This interference is characterized by the visualization of bright and dark spots which are called speckles (Briers et al., 2013). Figure 1 shows an example of a laser speckle image. The bright and dark spots can vary in size and shape, depending on the used sample, coherent light source and imaging system. This image has been sensitized using the algorithm detailed in (Kirkpatrick et al., 2007) and presents a situation with a speckle size of 8 pixels per speckle.

The laser speckle effect is widely used in biomedical applications as a tool to assess the blood perfusion (Briers et al., 2013). Its utilization fall from the idea that, when a moving scatterer is presented in the analysed sample, the speckle pattern will change over time. The temporal speckle variations encode information that can be related with the velocity of the dynamic scatterers. The analysis of laser speckle patterns over time is called dynamic laser speckle (Vaz et al., 2016a).

Normally, a two-dimensional imaging system, with finite exposure time, is used to record these speckle patterns along time resulting in a video struc-

ture. This information can be analysed by different ways. On one hand, these changes can be identified by comparing two consecutive speckle patterns. On the other hand, the speckle pattern can be analysed by computing its contrast using a method often called Laser Speckle Contrast Imaging (LSCI) (Draijer et al., 2009). The pattern contrast is related with the movement of the scatterers present in the sample. Faster scatterers mean faster image decorrelation leading to lower contrast (Briers and Webster, 1996).

When this technique is applied to biomedical samples, like cerebral tissue, the moving scatterers are mainly the red blood cells. As a consequence of the speckle behaviour, the contrast of the laser speckle pattern can be related with the tissue blood perfusion (Vaz et al., 2016b). The speckle contrast is usually computed in smaller regions of interest (ROI's) in order to achieve a two-dimensional contrast map. Laser speckle is able to produce two-dimensional perfusion maps in real-time (Humeau-Heurtier et al., 2013) and with frame rates above 100 frames per second (Tom et al., 2008) at a fair cost.

Speckle contrast can be computed using three different algorithms (Vaz et al., 2016b): the first one uses a spatial-based contrast computation, the second one uses a temporal-based computation and, finally, the last one combines the two previous families.

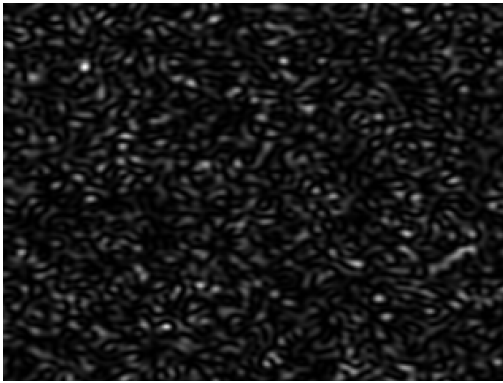


Figure 1: Synthetic laser speckle image with resolution of 320×240 pixels and a spot size of 8 pixels per speckle.

LSCI is used as a clinical and research tool in many different types of tissues and diseases. Most of the blood flow analyses performed with LSCI are related with highly vascularized tissues, like cerebral tissues (Kazmi et al., 2015), retinal tissues (Cheng and Duong, 2007) and hepatic tissues (Sturesson et al., 2013). However, more recently, the assessment of low vascularized tissues, like the skin, became also a major field of the application of LSCI (Humeau-Heurtier et al., 2013; Roustit et al., 2010). In this type of samples, studies on disorders like systemic sclerosis (Ruaro et al., 2013), port wine stains (Huang et al., 2009) and wound healing (Rege et al., 2012) have been performed using laser speckle imaging methods.

In this work, we propose to test the performance of a set of spatial-based contrast implementations. We will focus on this family because it is the most often used. When computing the contrast spatially a small two-dimensional ROI is used on the raw images. This ROI is translated along the laser speckle image (LS image) in the horizontal and vertical directions, generally without overlapping. Figure 2 presents an illustration of the spatial contrast algorithm.

The ROI is usually defined as a square of 3×3 (Pericam PSI documentation (Perimed AB, 2015)), 5×5 or 7×7 pixels (Draijer et al., 2009). The contrast is computed using the fundamental equation $K = \sigma(I)/\langle I \rangle$ where $\sigma(I)$ represents the standard deviation of the intensity and $\langle I \rangle$ the mean intensity within the ROI (Briers and Webster, 1996).

When online applications are necessary, or large images are analysed, computational speed is a key factor. The goal of this work is to explore different spatial contrast implementations in order to determine which one can achieve the best performance. This paper will aid researchers to select the suitable implementation depending on their requirements and to

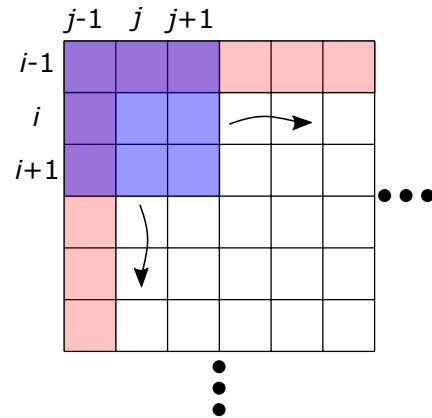


Figure 2: Schematic of spatial contrast algorithm. The blue square symbolizes a 3×3 ROI. Its contrast value is associated with the raw image pixel (i, j) . This ROI is translated along the lines and columns of the speckle image. The red lines correspond to boundary regions where contrast determination requires padding. Adapted from (Vaz et al., 2016b) with authors permission.

enlarge their implementations possibilities.

MATLAB[®] has been selected as a tool to test the different algorithm implementations. MATLAB[®] is a mathematical computing software, widely used in research for signal processing due to its rapid learning curve and large range of pre-implemented functions. The selected implementations, used to compute speckle contrast, correspond to methods presented in the literature (Steimers et al., 2016). Some implementations correspond to works previously performed (Duncan and Kirkpatrick, 2008; Steimers et al., 2016) and one corresponds to a novel implementation (subsection 2.4).

The performance results should be taken as specific for these experimental conditions, however these conclusions might be applied for other software and hardware platforms. The different implementations were tested using synthetic LS images produced using the method presented by Kirkpatrick *et al.* (Kirkpatrick et al., 2007).

2 METHODS

Four different implementations were developed in MATLAB R2016a-64 bits. The first one corresponds to an analytical evaluation of the contrast equation and was used as a reference. The second one is based on image filtering (Duncan and Kirkpatrick, 2008). The third one relies on a moving sums (Steimers et al., 2016). The fourth one uses convolution. The processing time of each implementation was analysed using different LS images and different ROI sizes.

LS images were synthesized with resolutions of 320×240 , 640×480 , and 1024×768 pixels and speckle sizes of 4, 8, 16, and 32 pixels. The applied ROI's have been defined as squares of 3×3 , 5×5 or 7×7 pixels. For each resolution, 200 different random generated images were used, 50 for each speckle size, and the computation time was determined as mean \pm standard deviation. The Floating-point Operations Per Second (FLOPS) were not computed because this command is no longer available in MATLAB after version R13SP2.

These images were filtered with an average filter in order to uniform their contrast. Figure 3 shows the global contrast distribution of the 600 images that were analysed in this work. This contrast exceeds the maximum theoretical laser speckle contrast due to the nature of the synthesis algorithm (Duncan and Kirkpatrick, 2008). None attempt has been made to correct this contrast overshoot in order to allow for other authors to follow the same protocol.

The first implementation (section 2.1) is based on the application of the contrast formula $K = \sigma(I)/\langle I \rangle$ to compute the output data. The other three (sections 2.2, 2.3, and 2.4) are based on a modified formula which replaces the standard deviation by intensity sums (Steimers et al., 2016):

$$K = \sqrt{\frac{N^2}{N-1} \times \frac{\sum I^2}{(\sum I)^2} - \frac{N}{N-1}}, \quad (1)$$

where N is the number of summed points. While the standard equation requires to compute both the mean and standard deviation of the ROI, equation (1) only requires to sum the pixels of the LS image and of its square. With this new equation, the spatial-contrast algorithm can be implemented in an optimized way.

The use of the modified contrast equation (Eq. (1)) presents a practical issue that should be discussed before its application. The square root operation can lead to imaginary values when its radicand is lower than 0. Rearranging the square root radicand we obtain that this equation is only valid if $\sum I^2 / (\sum I)^2 \geq 1/N$. This condition must be checked before the application of this equation.

2.1 Analytical Computation

The analytical computation corresponds to the direct application of the contrast equation in each ROI. The mean intensity and standard deviation in each ROI were computed using the functions `std2` and `mean2`. The ROI was applied to the entire LS image without overlapping, by using two `For` cycles (one for the rows and the other for the columns). The application

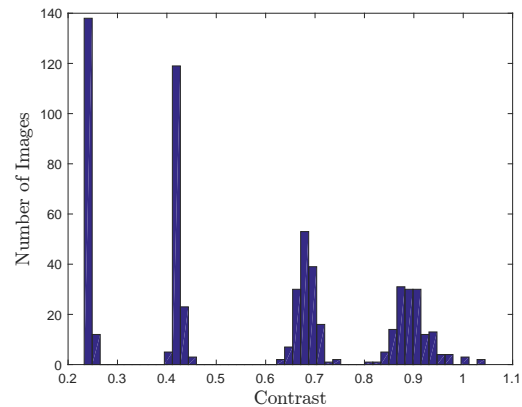


Figure 3: Distribution of the average contrast values of all the tested images. Total number of images: 600 frames.

of this process results in a reduction of the original image resolution depending on the ROI size. This implementation was not optimized and has been used as the reference method.

Algorithm 1: Analytical computation.

Input: LS raw image (*LSimage*) and element size (*ROIsize*)

Output: Contrast image (*cImage*)

for *ii* \leftarrow 1 **to** # of *LSimage* lines with *ROIsize* **steps**

do

for *jj* \leftarrow 1 **to** # of *LSimage* columns with *ROIsize* **steps**

do

ROI \leftarrow cut subimage with input size and the pixel center in the position (*ii*,*jj*)

mean \leftarrow `mean2(ROI)`

std \leftarrow `std2(ROI)`

contrast \leftarrow *std*/*mean*

cImage \leftarrow *contrast* is stored in the correct position of the *cImage*

end for

end for

return *cImage*

2.2 Filtering Implementation

The filtering implementation consists in the application of two images filters to the LS image. A regular filter, `imfilter`, with a kernel equal to the ROI was applied in order to compute the LS image sum and LS image squared sum. These data were then used to evaluate Eq. (1). The original implementation has been performed using MATLAB[®] (Duncan and Kirkpatrick, 2008). This implementation is detailed in pseudo-code in algorithm 2.

Algorithm 2: FILTERING.

Input: LS raw image ($LSimage$) and element size ($ROIsize$)
Output: Contrast image ($cImage$)
 $Kernel \leftarrow$ all-ones matrix with the $ROIsize$
 $Sum \leftarrow$ `imfilter`($LSimage$, $Kernel$)
 $Sum2 \leftarrow$ `imfilter`($LSimage^2$, $Kernel$)
 $cImage \leftarrow$ application of the sums equation for each point (Eq. 1)
return $cImage$

2.3 Moving Sum Implementation

The moving sum implementation has been described in (Steimers et al., 2016) and (Tom et al., 2008). The original algorithms were implemented in CUDA and C programming languages. Hence, an adaptation of this algorithm was implemented in MATLAB[®]. This implementation aims at computing the sums of Eq. (1) by performing a moving sum within the lines of the LS image and a moving sum in the columns of the resultant matrix. The moving sum was achieved by using the `movsum` function. This implementation is described in pseudo-code in algorithm 3.

Algorithm 3: MOVING SUM.

Input: LS raw image ($LSimage$) and element size ($ROIsize$)
Output: Contrast image ($cImage$)
 $SumLines \leftarrow$ `movsum`($LSimage$, $ROIsize$) for each line
 $SumLines2 \leftarrow$ `movsum`($LSimage.*LSimage$) for each line
 $Sum \leftarrow$ `movsum`($movSumLines$, $ROIsize$) for each column
 $Sum2 \leftarrow$ `movsum`($movSumLines2$, $ROIsize$) for each column
 $cImage \leftarrow$ application of the sums equation for each point (Eq. 1)
return $cImage$

2.4 Convolution Implementation

The two-dimensional convolution has been computed using `conv2` MATLAB[®] function. With this method, equation (1) can easily be computed. Both sums were computed by performing a convolution of the LS raw image with a all-ones matrix with size equal to the ROI. `conv2` uses the algorithm presented in equation (2). This MATLAB[®] function has also been tested against an equivalent method (convolution by fast Fourier transform) and presented the best results.

This implementation is described in pseudo-code in algorithm 4.

$$c(n1,n2) = \sum_{k1=-\infty}^{\infty} \sum_{k2=-\infty}^{\infty} I_1(k1,k2)I_2(n1-k1,n2-k2) \quad (2)$$

Algorithm 4: CONVOLUTION.

Input: LS raw image ($LSimage$) and element size ($ROIsize$)
Output: Contrast image ($cImage$)
 $Kernel \leftarrow$ all-ones matrix with size equals to $ROIsize$
 $Sum \leftarrow$ `conv2`($LSimage$, $Kernel$)
 $Sum2 \leftarrow$ `conv2`($LSimage.*LSimage$, $Kernel$)
 $cImage \leftarrow$ application of the sums equation for each point (Eq. 1)
return $cImage$

3 PERFORMANCE RESULTS

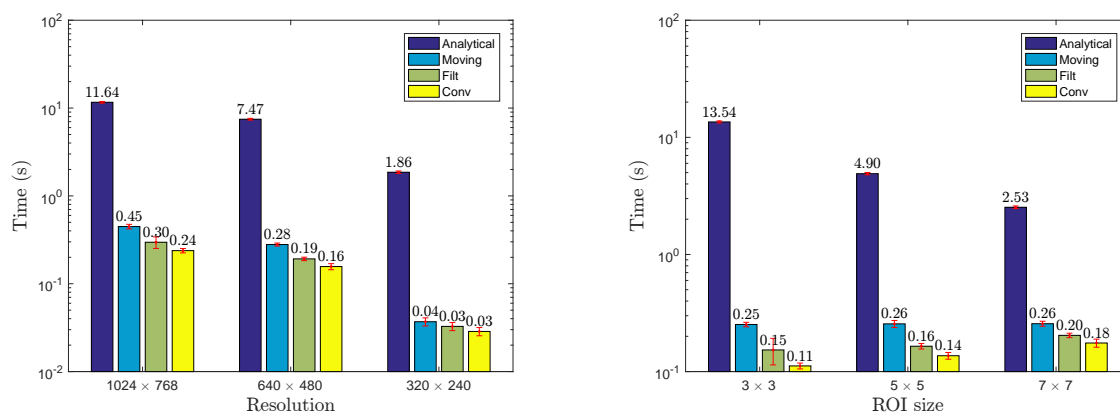
The results were analysed in terms of image resolution and ROI size. All the tests were performed in a computer Toshiba Tecra S11-11G - i7 M620 @ 2.67GHz with 4GB RAM with Windows 10 Pro as operating system. The results (figure 4) show that the convolution implementation achieves the best performance in all the cases, followed by the filtering algorithm.

The results are summarized in figure 4. This figure shows the computation time needed to process a single laser speckle frame in different conditions and with different implementations. Figure 4(a) presents the processing time as function of the image resolution and implementation. Figure 4(b) represents the processing time as function of the selected ROI size and implementation.

In general, the computation time decreases when the image resolution decreases. Regarding the ROI size, the computation time decreases for the analytical implementation but slightly increases for the other methods when the ROI size increases. The analytical computation presents the poorest performance, for a long margin, in all the tested cases. This was an expected result because this implementation have not been optimized in any form while the other have.

The moving sum (section 2.3) achieved the worst performance among the optimized implementations followed by the filtering implementation (section 2.2). Finally, the convolution implementation has achieved the best results.

The convolution implementation achieved a computational time which is approximately 50% lower than the one of the moving sum algorithm and two



(a) Each bar corresponds to the analysis of 600 images (200 for each ROI size).

(b) Each bar corresponds to the analysis of 600 images (complete data-set).

Figure 4: Analysis of the time required to process a single speckle image. The bars values correspondent to mean computation time needed to process one image laser speckle image. The error bars represented in red correspond to the standard deviation. The temporal axis (y) is represented in a logarithmic scale.

orders of magnitude lower than the analytical algorithm. It also gives better results than the ones obtained with the implementation proposed by Duncan and Kirkpatrick (Duncan and Kirkpatrick, 2008) (filtering) due to the optimization of the MATLAB[®] function `conv2`. In this comparison, the performance improvement is more visible for smaller ROI. In the case of a ROI size equals to 3×3 pixels, the convolution algorithm achieved a computational time $\approx 26\%$ lower than the filtering implementation.

All the optimized implementations present result of, at least, two orders of magnitude lower than the reference method (analytical). This result is explained by an absence of optimization of the analytical implementation.

4 CONCLUSION

Most papers using laser speckle imaging algorithm optimization are performed using graphic processing units (GPUs) (Liu et al., 2008). However, implementation efficiency is highly dependent on the programming software used and can also be performed by dedicated hardware. For this reason, there is no gold standard implementation. Tom *et al.* (Tom et al., 2008) presented an important overview of several algorithms but applied to C programming language.

The proposed implementations, except for the analytical one, are able to compute the contrast map with overlapping ROI without increasing the computation time. Their application results in a contrast matrix with the same resolution as the original image (excluding the boundary constraints). The absence of

overlapping is obtained by selecting the central point of each ROI.

In our conditions, the new proposed convolution algorithm achieves the best performance in all the tests. The convolution method is simple and is present in many image processing fields. The advantage of this implementation over complex methods is that high-performance FPGA-based implementations can be found in literature (Perri et al., 2005; Carlo et al., 2011). Since the used hardware platform and programming style are extremely variable, this note should be used as a guideline for other implementations rather than as a rule.

ACKNOWLEDGEMENTS

This work was partly supported by Fundação para a Ciência e Tecnologia (FCT) with a doctoral scholarship (SFRH/BD/89585/2012) and project IF/01238/2013.

REFERENCES

- Briers, D., Duncan, D., Kirkpatrick, S., Larsson, M., Stromberg, T., and Thompson, O. (2013). Laser speckle contrast imaging : theoretical and practical limitations. *J. Biomedical Opt.*, 18(6):1–9.
- Briers, J. and Webster, S. (1996). Laser speckle contrast analysis (LASCA): A non-scanning, full-field technique for monitoring capillary blood flow. *J. Biomed. Opt.*, 1(2):174–179.
- Carlo, S. D., Gambardella, G., Indaco, M., Rolfo, D., Tiotto, G., and Prinetto, P. (2011). An area-efficient

- 2-D convolution implementation on FPGA for space applications. In *IEEE 6th Int. Des. Test Work.*, pages 88–92. IEEE.
- Cheng, H. and Duong, T. Q. (2007). Simplified laser-speckle-imaging analysis method and its application to retinal blood flow imaging. *Opt. Lett.*, 32(15):2188–2190.
- Draijer, M., Hondebrink, E., van Leeuwen, T., and Steenbergen, W. (2009). Review of laser speckle contrast techniques for visualizing tissue perfusion. *Lasers Med. Sci.*, 24(4):639–651.
- Duncan, D. and Kirkpatrick, S. (2008). Spatio-temporal algorithms for processing laser speckle imaging data. In *Opt. Tissue Eng. Regen. Med. II*, number February, pages 685802–685802–6. International Society for Optics and Photonics.
- Huang, Y., Tran, N., Shumaker, P. R., Kelly, K., Ross, E. V., Nelson, J. S., and Choi, B. (2009). Blood flow dynamics after laser therapy of port wine stain birthmarks. *Lasers Surg. Med.*, 41(8):563–571.
- Humeau-Heurtier, A., Guerreschi, E., Abraham, P., and Mahé, G. (2013). Relevance of laser Doppler and laser speckle techniques for assessing vascular function: State of the art and future trends. *IEEE Trans. Biomed. Eng.*, 60(3):659–666.
- Kazmi, S. M. S., Richards, L. M., Schrandt, C. J., Davis, M. a., and Dunn, A. K. (2015). Expanding applications, accuracy, and interpretation of laser speckle contrast imaging of cerebral blood flow. *J. Cereb. Blood Flow Metab.*, 35(7):1076–1084.
- Kirkpatrick, S., Duncan, D., Wang, R., and Hinds, M. (2007). Quantitative temporal speckle contrast imaging for tissue mechanics. *J. Opt. Soc. Am. A. Opt. Image Sci. Vis.*, 24(12):3728–3734.
- Liu, S., Li, P., and Luo, Q. (2008). Fast blood flow visualization of high-resolution laser speckle imaging data using graphics processing unit. *Opt. Express*, 16(19):2188–2190.
- Perimed AB (2015). Pericam psi sytem. <https://www.perimed-instruments.com/products/pericam-psi>.
- Perri, S., Lanuzza, M., Corsonello, P., and Cocorullo, G. (2005). A high-performance fully reconfigurable FPGA-based 2D convolution processor. *Microprocess. Microsyst.*, 29(89):381–391.
- Rege, A., Thakor, N., Rhie, K., and Pathak, A. (2012). In vivo laser speckle imaging reveals microvascular remodeling and hemodynamic changes during wound healing angiogenesis. *Angiogenesis*, 15(1):87–98.
- Roustit, M., Millet, C., Blaise, S., Dufournet, B., and Czacowski, J. L. (2010). Excellent reproducibility of laser speckle contrast imaging to assess skin microvascular reactivity. *Microvasc. Res.*, 80(3):505–511.
- Ruaro, B., Sulli, A., Alessandri, E., Pizzorni, C., Ferrari, G., and Cutolo, M. (2013). Laser speckle contrast analysis: a new method to evaluate peripheral blood perfusion in systemic sclerosis patients. *Ann. Rheum. Dis.*, pages annrheumdis–2013.
- Steimers, A., Farnung, W., and Kohl-Bareis, M. (2016). Improvement of Speckle Contrast Image Processing by an Efficient Algorithm BT - Oxygen Transport to Tissue XXXVII. pages 419–425. Springer New York, New York, NY.
- Sturesson, C., Milstein, D. M. J., Post, I. C. J. H., Maas, A. M., and van Gulik, T. M. (2013). Laser speckle contrast imaging for assessment of liver microcirculation. *Microvasc. Res.*, 87:34–40.
- Tom, W. J., Ponticorvo, A., and Dunn, A. K. (2008). Efficient processing of laser speckle contrast images. *Med. Imaging, IEEE Trans.*, 27(12):1728–1738.
- Vaz, P., Pereira, T., Figueiras, E., Correia, C., Humeau-Heurtier, A., and Cardoso, J. (2016a). Which wavelength is the best for arterial pulse waveform extraction using laser speckle imaging? *Biomed. Signal Process. Control*, 25:188–195.
- Vaz, P. G., Humeau-Heurtier, A., Figueiras, E., Correia, C., and Cardoso, J. (2016b). Laser speckle imaging to monitor microvascular blood flow: a Review. *IEEE Rev. Biomed. Eng.*, In press(99):1–1.